PERGAMON

Energy Conversion & Management 40 (1999) 1423–1439

ENERGY CONVERSION & MANAGEMENT

Solar desalination based on humidification process—I. Evaluating the heat and mass transfer coefficients

Naser Kh. Nawayseh[a,*], Mohammed Mehdi Farid[b], Said Al-Hallaj[c], Abdul Rahman Al-Timimi[c]

[a]*School of Industrial Technology, University Sains Malaysia, 11800, Penang, Malaysia*
[b]*Department of Chemical & Material Engineering, The University of Auckland, Auckland, New Zealand*
[c]*Department of Chemical Engineering, Jordan University of Science & Technology, Irbid, Jordan*

Received 23 April 1998; accepted 21 December 1998

Abstract

Solar desalination with a humidification–dehumidification process has proven to be an efficient means of utilizing solar energy for the production of fresh water from saline or sea water. The process used in this work is a closed air cycle type, in which air is circulated in the unit by natural draft between the humidifier and condenser.

In order to scale up a unit of this type, it is necessary to obtain sufficient information on the process of heat and mass transfer in the unit. The humidifier and the condenser had to be specially designed to maintain minimum pressure drop in the unit. The mass transfer coefficient in the humidifier was found to be affected mostly by the water flow rate due to its effect on the wetting area of the packing. In natural draft operation, the air circulation rate was found to increase with water flow rate, causing a further increase in the mass transfer coefficient. It was possible to predict and correlate the mass and heat transfer coefficients in the humidifiers and condensers, having different designs, in the three units constructed by us in Jordan and Malaysia.

Keywords: Solar; Desalination; Humidification

* Corresponding author. Present address: Department of Automatic Control and Systems Engineering, The University of Sheffield, Mappin Street, Sheffield S1 3JD, UK. Fax: +44-114-273-1729.
E-mail address: COP98NKN@sheffield.ac.uk (N.Kh. Nawayseh)

0196-8904/99/$ - see front matter
PII: S0196-8904(99)00018-7

Nomenclature

A	surface area of condenser (m^2)
a	wetted area (m^2/m^3)
Cp	specific heat capacity (J/kg K)
D	copper pipe diameter (m)
D_H	hydraulic diameter in Re and Nu numbers (m)
d	characteristics dimension in Gr and Gz numbers (m)
η	fin efficiency
G	air mass flow rate (kg/s)
Gr	$\frac{\rho^2 g\beta(T_w-T_a)d^\beta}{\mu^2 f}$, Grashof number (dimensionless)
Gz	$Re\ Pr\frac{d}{L_u}$, Graetz number (dimensionless)
g	gravity acceleration (m/s^2)
H	enthalpy of saturated air (kJ/kg dry air)
h_a	air side convection heat transfer coefficient (W/m^2 K)
h_c	condensation coefficient with non-condensable air (W/m^2 K)
h_w	water side heat transfer coefficient (W/m^2 K)
K	mass transfer coefficient (kg/m^2 s)
k	thermal conductivity (W/m K)
L	water mass flow rate (kg/s)
L_f	characteristic fin dimension
L_u	height of unit (m)
L'	water mass velocity (kg/m^2 s)
I	pipe length (m)
Nu	$\frac{h_a D_H}{k}$, Nusselt number (dimensionless)
Pr	$\frac{Cp\mu}{k}$, Prandtl number (dimensionless)
Re	$\frac{\rho v D_H}{\mu_f}$, Reynolds number (dimensionless)
T	temperature (°C)
U	theoretical overall heat transfer coefficient (W/m^2 K)
U_{exp}	experimental overall heat transfer coefficient (W/m^2 K)
V	volume of humidifier (m^3)
Z	ratio of sensible to total heat (dimensionless)

Greek

$(\Delta T)_{lm}$	log mean temperature difference (°C)
μ	dynamic viscosity (kg/m s)
ρ	density (kg/m^3)
η	fin efficiency (dimensionless)

Subscript

1	water inlet to condenser
2	water outlet from condenser

3	water inlet to humidifier
4	water outlet from humidifier
5	air at bottom of unit
6	air at top of unit
a	air
b	bulk
c	condenser
cyl	condenser cylinder
f	fin, or condition at air–water interface
t	tube
w	water, or condition at wall

1. Introduction

Water is available in abundant quantities in nature, however, there is a shortage of potable water in many countries in the world. Expensive non-renewable energy, such as petroleum fuel and natural gas, has been used in the Gulf for water desalination either directly or through its conversion to electricity, which may be used to run reverse osmosis units.

The fact that the shortage of water occurs at places of hot climate with high solar radiation may make the application of solar energy for water desalination practical. This has been the attempts of many investigators since many years, using single or multiple-basin stills. The efficiency of these stills is of the order of 30–50% only, which is due to the large heat losses through the glass cover of the still, where the condensation occurs.

If a flat plate solar collector is used to provide the heat, then the maximum water temperature should not exceed 70° to 80°C, otherwise the collector efficiency will drop significantly. Water at such temperatures requires an efficient method of evaporation, such as spraying over some packing against countercurrent air flow. This led to the development of a desalination process known as the multi-effect humidification–dehumidification process (MEH).

It has been shown [1] that the humidification–dehumidification process could be an efficient and economical method of solar desalination. The process is based on humidifying air, circulated in a closed loop, using hot water obtained from a flat plate solar collector. The hot humidified air is partially condensed in a large surface condenser, producing low salinity water. The successful feature of the process lies in its ability to utilize the latent heat of condensation by preheating the feed saline water. Such units produce desalinated water at rates higher than those usually obtained from single basin solar stills under similar solar radiation [1]. Moreover, the unit produces also a large quantity of warm water which can be utilized for some domestic purposes. This suggests that such a process could be practical for desalination of water when the warm water leaving the unit can be utilized for other domestic uses.

Two units of different sizes were constructed and operated in Jordan in steady state and unsteady state operations [1]. The pilot unit was 2 m in height and was constructed from galvanized steel plates, while the bench scale unit was only 1 m in height and was constructed from Plexiglas. Both of the units consisted of two vertical rectangular ducts connected at their upper and lower ends to form a closed loop for air circulation. In one of the ducts, a large

surface condenser was fixed, while the other duct contained a large number of wooden slats fixed in a wooden frame to form a typical humidifying tower. A third unit was constructed in Malaysia, based on the same process. That unit was 3 m in height and was constructed from PVC pipes. The outside and inside diameters of the pipe were 316 and 295 mm, respectively. Details of this unit are given by Nawayseh [2].

The hot water leaving the flat plate solar collector was sprayed on the packing using a simple distributor. The concentrated brine was rejected from the bottom of the humidifier section, while the desalinated water was withdrawn from the bottom of the condenser section. The air was circulated in the unit either by natural draft or forced draft, using an electrical fan fixed at the upper section of the two units constructed in Jordan. The three units were operated in a steady state mode using an electrical heater and in an unsteady state mode using solar energy for heating the water. However, only the steady state, well controlled measurements, were used in the study of the heat and mass transfer in the units. Fig. 1 shows a sketch of the desalination process.

Most of the previous investigators on the MEH units [1,3,4–7] reported productivity significantly higher than those of the single basin still. The large variation in the productivity of the different MEH units reported in the literature suggests that the design of some of these units was far from optimum. The effect of some parameters, such as water flow rate, on the production rate was complicated by its combined effects on the performance of the condenser, humidifier and solar collector.

The design of any MEH unit requires an accurate analysis of the heat and mass transfer in

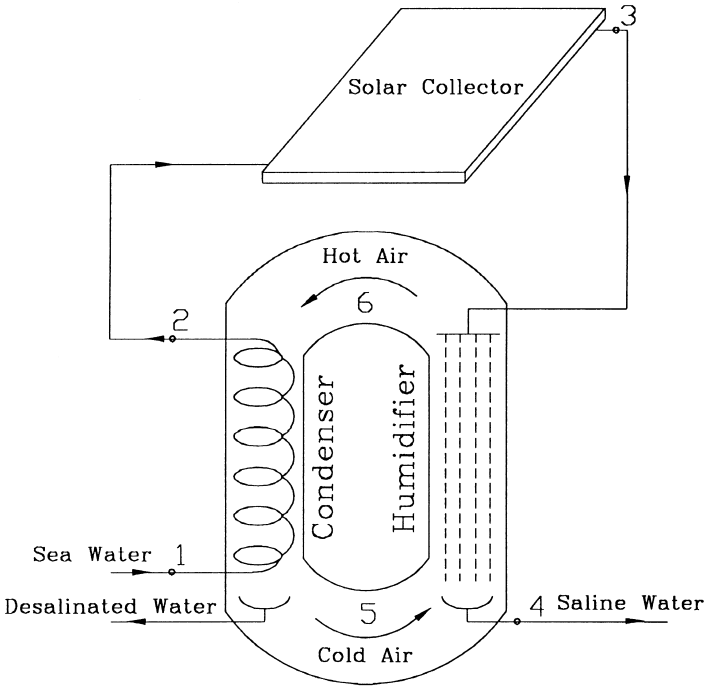

Fig. 1. Sketch of the desalination process.

the humidifier and condenser. The mass transfer coefficient in the humidifier is expected to be different from the values reported in the literature [8] for cooling towers. Cooling towers are usually operated with water temperatures below 50°C, and most of the correlations developed were based on that. This is the maximum temperature allowed for the water leaving industrial heat exchangers to avoid corrosion problems. Further, the air enters the humidifier in the MEH units fully saturated, unlike what is usually found in cooling towers.

The condensers used in the desalination units were of special design, as will be discussed in this paper. The mass transfer resistance, due to condensation of water vapor in the presence of stagnant air, complicates the evaluation of the heat transfer coefficient in the condenser. The third component of the desalination unit is the flat plate solar collector. The performance and efficiency of the collector are easily evaluated as shown by solar energy textbooks, such as that of Hsieh [9], and, hence, will not be discussed in this paper.

The correlation for the heat and mass transfer coefficients developed in this paper will be used in the simulation work presented in part II of the work.

2. Performance of the desalination unit under steady state operation

Figs. 2 and 3 show the productivity of the three desalination units under steady state

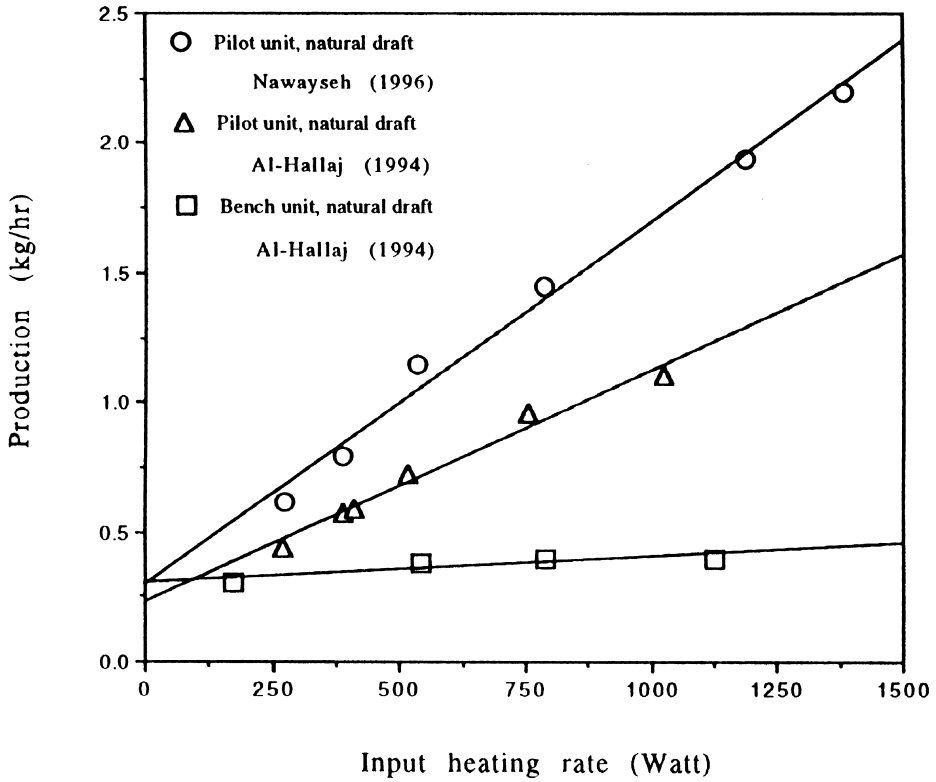

Fig. 2. Desalination production rate for the different desalination units.

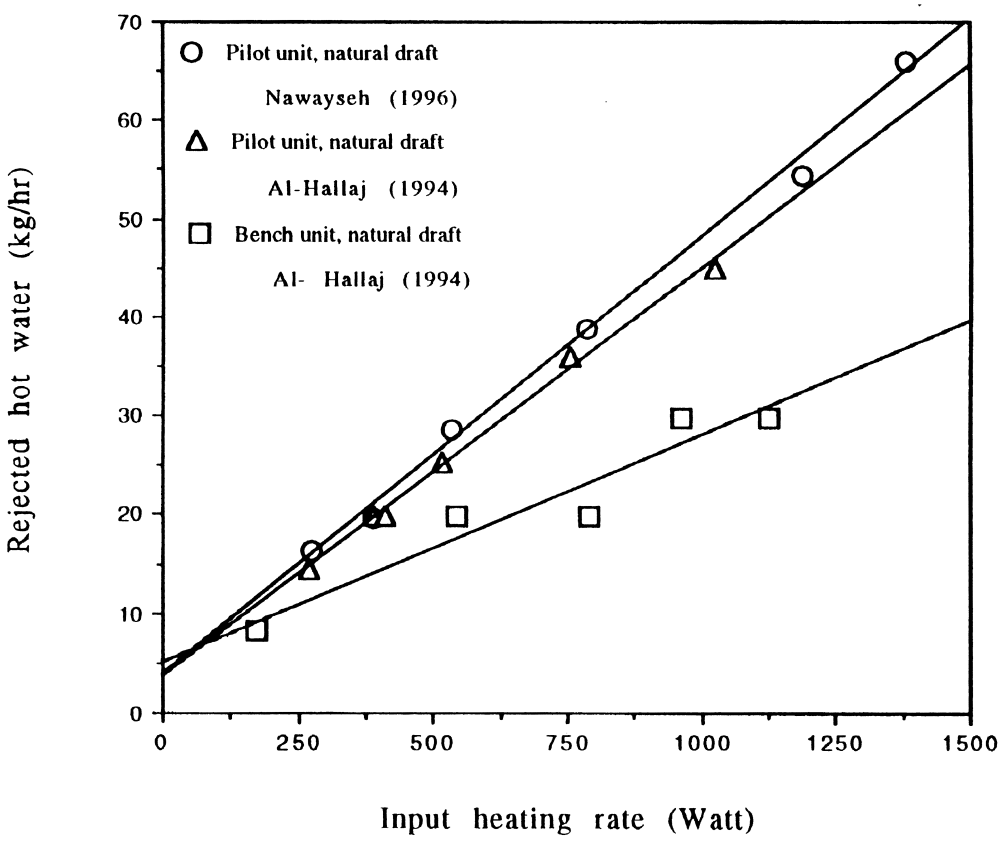

Fig. 3. Hot water production at about 40°C, for the different desalination units.

operation using electrical heating to heat the water leaving the condenser. For 1.0 kW heating power, Fig. 2 shows that the unit constructed in Malaysia may produce 1.7 kg/h of desalinated water, and Fig. 3 shows that the same unit is capable of producing about 50 kg/h of warm water at about 40°C. These figures also show that the productivity of desalinated water was significantly improved in the unit constructed in Malaysia in comparison to that built in Jordan. This is due to the larger contact area of the humidifier and condenser of the unit constructed in Malaysia. The percentage increases of the humidifier, single condenser and double condenser areas were 136, 122.5 and 11.25%, respectively. The warm water production was found similar in the two pilot units, since it is only a function of the heat input to the unit and the heat losses through the insulation.

3. Mass transfer coefficient in the humidifier

The humidifier was a typical cooling tower with wooden slats packing, as shown in Fig. 4. In the two units constructed in Jordan, the wooden slats were fixed in a wooden rectangular frame with an inclination of 45° in multiple rows along the whole height of the frame. The

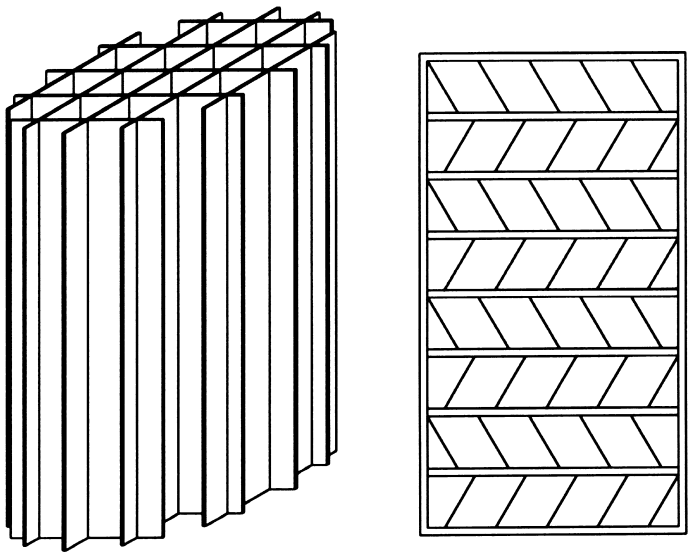

a. Nawayseh (1996). b. Al-Hallaj (1994).

Fig. 4. Sketch of the different wooden packing used in the humidifiers.

dimensions of the frame in the pilot and bench units were $1.0 \times 0.18 \times 2.0$ m and $0.3 \times 0.05 \times 1.0$ m, respectively. These dimensions provided packing surface areas of 14 m^2/m^3 for the pilot unit and 87 m^2/m^3 for the bench unit, with a minimum air pressure drop. The true surface area of the packing in the pilot and bench units were 5.04 m^2 and 0.96 m^2, respectively. In the 3 m high unit, constructed in Malaysia, the packing was made of wooden thin sheets combined in cross arrangement to form six modules of 0.5 m height, as shown in Fig. 4. The modules were dropped from the top of the unit to form the 3 m height humidifier. The arrangements gave a packing surface area of 11.9 m^2 (58 m^2/m^3).

It is common practice in the design of cooling towers to use the performance characteristic, KaV/L, defined as follows

$$KaV/L = \int_{T_4}^{T_3} \frac{C\mathrm{p_w} \mathrm{d}T}{H_\mathrm{f} - H_\mathrm{a}} \tag{1}$$

where K is a mass transfer coefficient (kg water evaporated/m^2 s) and a is the surface area of packing per unit volume. The integral may be evaluated from the measured temperatures and enthalpies of the water and air entering and leaving the humidifier. If the operating range of the temperature is small enough to allow the assumption of a linear enthalpy-temperature saturation line, then the log mean driving force $(H_\mathrm{f} - H_\mathrm{a})_\mathrm{lm}$ may be used for evaluation of the integral, otherwise numerical integration will be necessary. The point to point calculation will increase significantly the computation time in the simulation program described in part II of this work. Hence, it was decided to employ the log mean enthalpy as a driving force.

In each run, the electrical heating power and water flow rate were set to the desired values. In the forced air circulation mode, different air velocities were obtained by applying a variable

AC power supply to the fan. Then, the desalination unit was left running for a few hours to reach steady state. The humidity of the air at the top and bottom of the unit were measured and found saturated. The inlet and outlet temperatures of the condenser, humidifier and solar collector were measured. The air temperature at the top and bottom of the unit, as well as the ambient temperature, were measured. The temperature measurements were made using thermocouples and multi-channel programmable recorder/data acquisition units. The water inlet flow rate was measured using a rotameter, while the brine and desalinated water flow rates were measured by graduated cylinder.

It was not possible to measure the velocity of the air using a hot wire anemometer because of the strong effect of humidity on the measurements. In the natural draft air circulation, the air velocity was too small to be measured accurately by any available method. It was decided to calculate the air velocity from the energy balance over the condenser and the humidifier:

$$G(H_6 - H_5) = LC\mathrm{p}_\mathrm{w}(T_2 - T_1) + \text{Losses} \tag{2}$$

$$G(H_6 - H_5) = LC\mathrm{p}_\mathrm{w}(T_3 - T_4) - \text{Losses} \tag{3}$$

Adding the above two equations eliminates the heat loss term, assuming similar heat losses through the walls of the condenser and the humidifier. The following expression was used to define the enthalpy of the saturated air, as derived from the data given by Stoecker

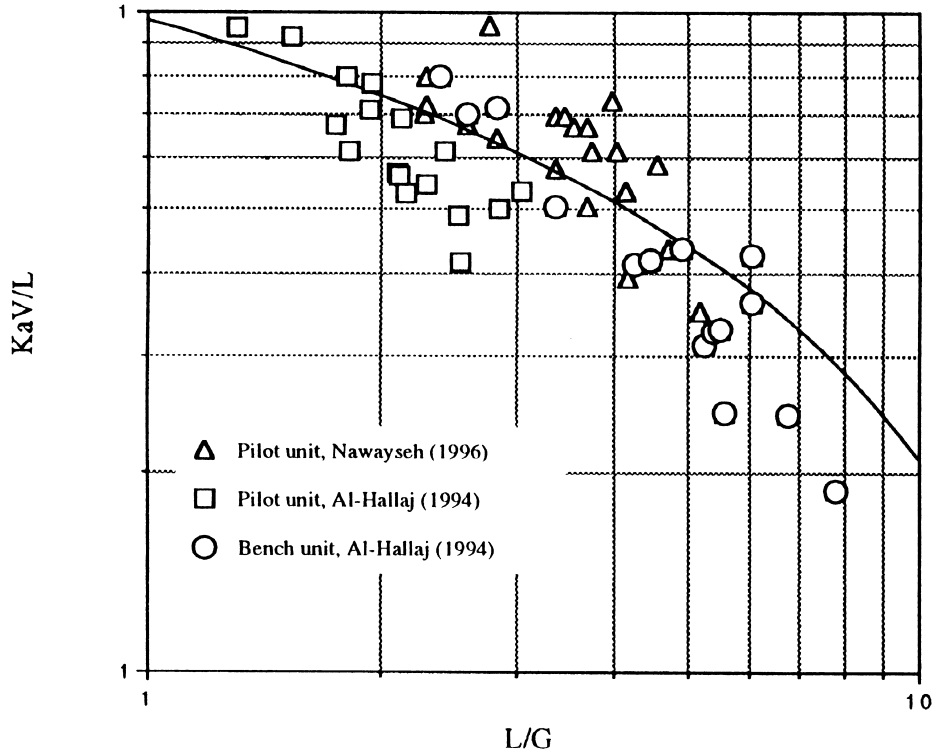

Fig. 5. Mass transfer coefficient in the different humidifiers with natural draft air circulation.

and Jones [10]:

$$H = 0.005853T^3 - 0.497T^2 + 19.87T - 207.61 \quad (4)$$

where T is the air dry bulb temperature in °C.

The effect of L/G on the mass transfer characteristic KaV/L is shown in Fig. 5 for natural draft operation for the three desalination units investigated. In spite of the large variation in the dimensions of the units, the mass transfer coefficient in these units correlates well and could be described by a single correlation. However, the values obtained from the unit constructed in Malaysia were generally higher due to a larger value of the humidifier packing area aV. Fig. 6 shows a similar plot for the forced draft air circulation obtained from the pilot unit constructed in Jordan. The effect of L/G is very different in the two modes of operation. Fig. 6 shows a weak dependence of KaV/L on air flow rate within the allowable operating range. This may explain the result of no significant improvement in the productivity of the desalination unit when forced air circulation was used. The strong dependence of KaV/L on G, shown in Fig. 5, is due to the fact that the air flow rate in the natural draft operation is directly proportional to the water flow rate, as may be seen from the heat balance. Hence, the effect shown in Fig. 5 is solely due to water flow rate alone.

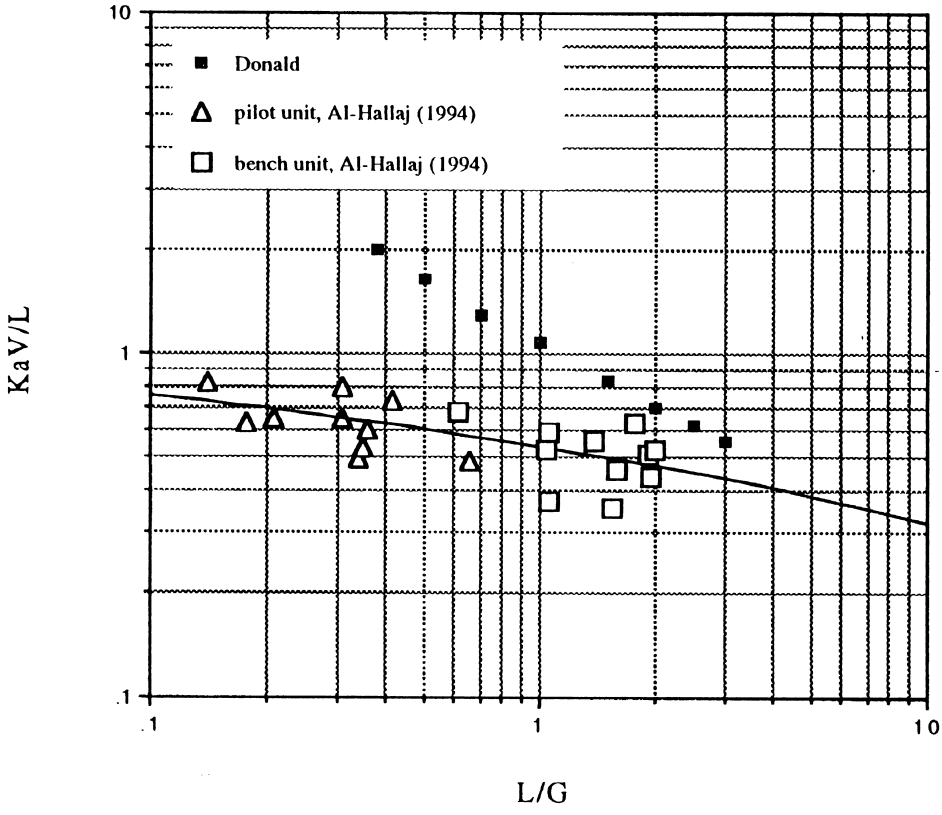

Fig. 6. Mass transfer coefficient in the different humidifiers with forced draft air circulation.

Fig. 6 shows that the water flow rate has a strong effect on the volumetric mass transfer coefficient KaV. However, Fig. 5 does not clearly depict the effect of water flow rate on KaV due to the dependence of G on L in the natural air draft operation. Hence, it was decided to plot KaV against L rather than L/G for this mode of operation. Fig. 7 shows the strong dependence of KaV on L for the three units. This strong dependence is well recognized previously [8] and is believed to be due to the effect of water flow rate on the wetted area of the packing.

The following correlations were found from the best fit to the data of Figs. 5 and 6:

$$KaV/L = 0.97 - 0.76\log(L/G) \quad \text{for natural draft} \quad 1<L/G<8 \tag{5}$$

$$KaV/L = 0.53 - 0.22\log(L/G) \quad \text{for forced draft} \quad 0.1<L/G<2 \tag{6}$$

or in the more conventional way:

$$KaV/L = 1.19(L/G)^{-0.66} \quad \text{for natural draft} \quad 1<L/G<8 \tag{5'}$$

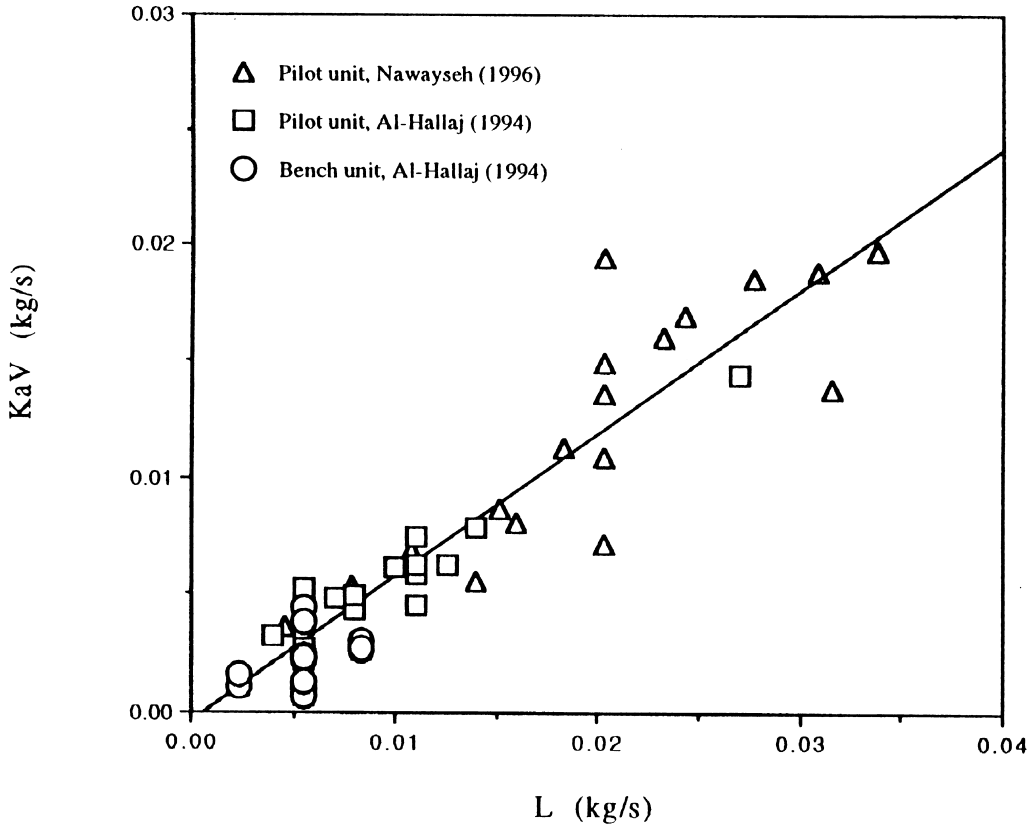

Fig. 7. Effect of water flow rate on the mass transfer coefficient in the humidifiers.

$$KaV/L = 0.52(L/G)^{-0.16} \quad \text{for forced draft} \quad 0.1<L/G<2 \tag{6'}$$

The previous correlation presented by Farid et al. [11], based on the two units constructed in Jordan, gives lower values of mass transfer coefficient when compared to Eq. (5). The shown scatter is expected, as the humidifiers in the three units were of different sizes and the packing used had different surface areas. The variation in the operating temperature also plays a significant role in increasing the scatter. Fig. 6 includes some measured KaV/L in industrial cooling towers as presented by Donald [8]. The reported coefficient is much higher than that measured in this work, especially at low values of L/G. This is believed to be due to the low water flow rate employed in the desalination unit compared to that usually employed in industrial cooling towers.

It is known that most of the heat and mass transfer resistance lies in the gas film rather than in the liquid film in any humidification process. Then, the strong effect of the water flow rate on the volumetric mass transfer coefficient Ka must be due to its effect on the degree of wetting of the packing. If the mass transfer coefficient (evaporative coefficient) is calculated theoretically, then the true wetted area may be estimated by dividing the measured Ka by the theoretically calculated area coefficient K. The following equation was used to calculate the convection heat transfer coefficient in the units when forced air circulation was used:

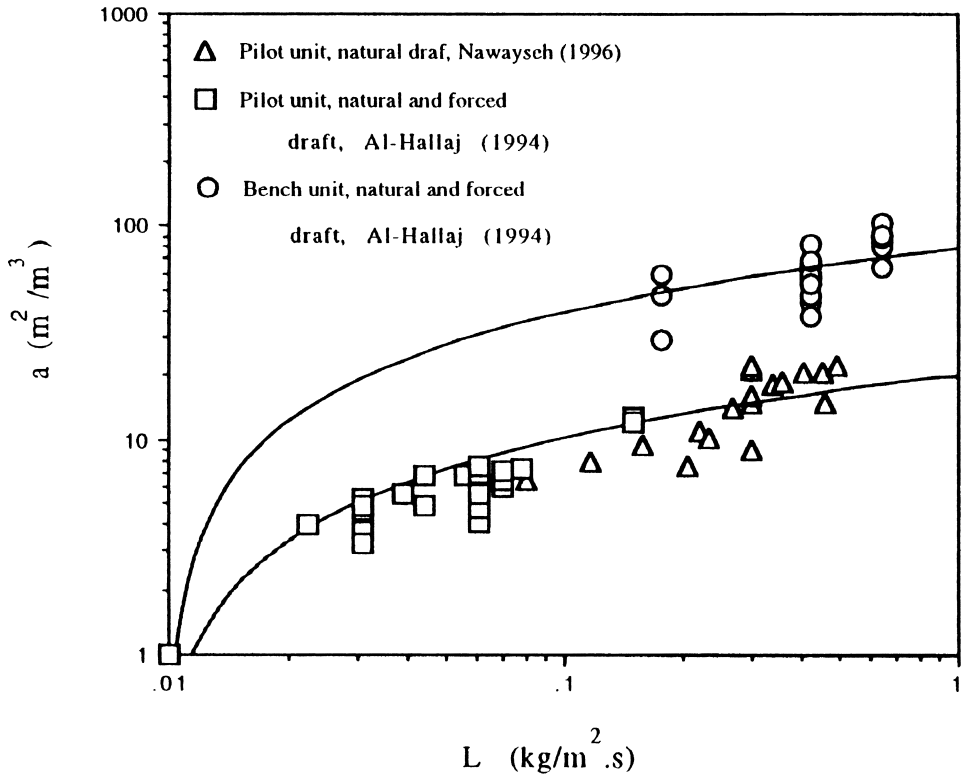

Fig. 8. Effect of water mass velocity on the wetting area of the different packing.

$$Nu = 1.75\left(\frac{\mu_b}{\mu_w}\right)^{0.14}\left[Gz + 0.012(Gz\ Gr^{1/3})^{4/3}\right]^{1/3} \tag{7}$$

The above equation was based on the analysis of mixed convection heat transfer [12]. The characteristic dimension used in the *Re* and *Nu* numbers is the hydraulic diameter of the flow area enclosed by the adjacent wooden slats. The distance between the wooden slats was used as the characteristic dimension in the Grashof number. The same equation was found to predict the coefficient during the natural draft circulation in the small unit. However, it was not applicable to the condition of natural draft in the pilot units due to the extremely low air velocities. The coefficient was found to be of the order of two times that found from the above equation. The mass transfer coefficient was calculated based on the Lewis relationship as defined by Donald [8]:

$$K = \frac{h_a}{C_{p_a}} \tag{8}$$

Fig. 8 shows the calculated values of the wetting area per unit volume during natural and forced draft operations for the three units. As the water mass velocity increased, the wetted area approached the true total surface area of the packing in the three units which were 14 m^2/m^3 and 87 m^2/m^3 for the pilot and bench units constructed in Jordan and was 58 m^2/m^3 for the unit constructed in Malaysia. In the two pilot units, the effective area was only 50% of the true area even at the maximum flow rate used. This is due to the oversized cross sectional area of the humidifier and the low water flow rate used. Although the humidifier cross sectional area in the unit constructed in Malaysia was reduced by 39% of that of the unit constructed in Jordan, complete wetting has not been achieved due to the use of vertical wooden slats which have less chance of wetting than the inclined slats.

4. Heat transfer in the condenser

In order to utilize the latent heat of condensation of water efficiently, the condenser area must be made large. The overall heat transfer coefficient of the condenser is expected to be small due to:

1. The low velocity of the air circulated in the unit, even in forced circulation which was necessary to avoid excessive pressure drop.
2. The large reduction in the condensation heat transfer coefficient due to the mass transfer resistance occurring in the process of condensation of water vapor with non-condensable air.
3. The low water side heat transfer coefficient due to the low water flow rate per unit condenser area. However, a small diameter tube was used to overcome this problem.

In the desalination units constructed in Jordan, the condensers were constructed from 1.0×0.3 and 2.0×1.0 m galvanized steel plates for the bench and pilot units, respectively. In the pilot unit, a copper tube having 11 mm OD and 18 m long was welded to the galvanized plate in a helical shape. The tube outside diameter and length in the bench unit were 8 mm and 3 m,

respectively. Either one or two condensers, connected in series, were fixed vertically in one of the ducts in both units. Fig. 9 shows sketches of the condensers used in the units constructed in Malaysia and Jordan.

In the pilot unit constructed in Malaysia, the condenser was simply a 3 m long cylinder

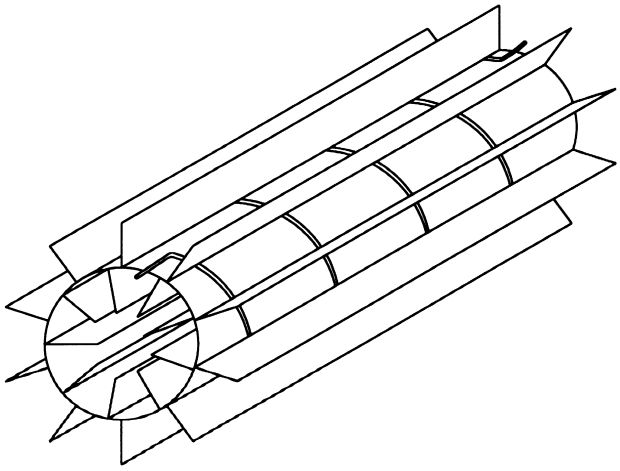

a. Nawayseh (1996).

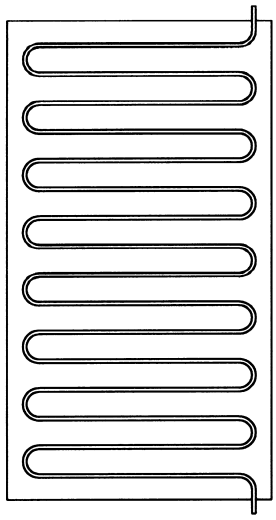

b. Al-Hallaj (1994).

Fig. 9. Sketch of the different condensers used in the desalination units.

having a diameter of 170 mm and made of galvanized steel plates. Ten longitudinal fins were soldered to the outer surface of the cylinder and nine similar fins were soldered to the inner surface. The height of the inside and outside fins was 50 mm. The thickness of the plate used to make the cylinder and the fins was 1.0 mm. A 19.2 m long copper tube having 9.5 mm inside diameter was soldered to the surface of the cylinder. The condenser was fixed vertically in the 316 mm diameter PVC pipe which is connected to the humidifier section by two short horizontal PVC pipes.

The following expression was used to define an overall heat transfer coefficient for the condenser used in the unit constructed in Jordan, based on series resistance. The contact resistance between the copper tube and the condenser surface was assumed negligible.

$$\frac{1}{UA_c} = \frac{1}{h_w A_t} + \frac{1}{\eta_c A_c h_c} \tag{9}$$

For the condenser constructed in Malaysia, heat flows from the humid air to the cooling water either through the fins or through the cylinder itself. These two heat flow paths may be represented by the following two resistances;

$$R_1 = \frac{1}{h_w A_t} + \frac{1}{\eta_f A_f h_c} \tag{10}$$

$$R_2 = \frac{1}{h_w A_t} + \frac{1}{\eta_f A_{cyl} h_c} \tag{11}$$

Then, the overall heat transfer resistance may be defined as follows, assuming parallel resistances;

$$UA_c = \frac{1}{R_1} + \frac{1}{R_2} \tag{12}$$

The fin efficiency η_f is the usual fin efficiency defined in the heat transfer textbooks:

$$\eta_f = \frac{\tanh \sqrt{\frac{2h_c}{kt}} L_f}{\sqrt{\frac{2h_c}{kt}} L_f} \tag{13}$$

The characteristic fin dimension L_f was taken equal to half the tubes spacing in Eq. (10) and (12). For the true fin in Eq. (11), it was taken equal to the true fin height plus half the tubes spacing, as may be seen from the two heat flow paths.

The air side heat transfer coefficient *hc* is a condensation coefficient that includes a significant mass transfer resistance due to the presence of the non-condensable air. The values of *hc* vary along the condenser height, and hence, a point to point calculation is required [13]. However, in order to obtain an average value to be used in the simulation, the approximate analysis [14] was followed. In this method, the coefficient *hc* is defined as follows:

$$hc = ha/Z \tag{14}$$

where *ha* is the convection heat transfer coefficient of the humid air flowing along the condenser surface by forced or free convection. The same empirical correlation, Eq. (7), was used to calculate the convection heat transfer coefficient *ha*.

The condensation factor Z represents the ratio of the sensible to the total heat load in the condenser:

$$Z = C\mathrm{p}_a \mathrm{d}T/\mathrm{d}H \tag{15}$$

Values of Z were obtained from the derivative of the enthalpy expression defined by Eq. (4), calculated at the average operating temperature. The above equations show that the condensation coefficient may vary from two to eight times that of the convection coefficient, depending on the operating temperature. In fact, the condensation heat transfer coefficient defined by Eq. (14) is the same coefficient calculated based on the Lewis relationship. If the values of K obtained from Eq. (8) are multiplied by $\Delta H/\Delta T$, it will give the evaporative heat transfer coefficient which, on addition to the convection coefficient, will give the total heat transfer coefficient *hc*.

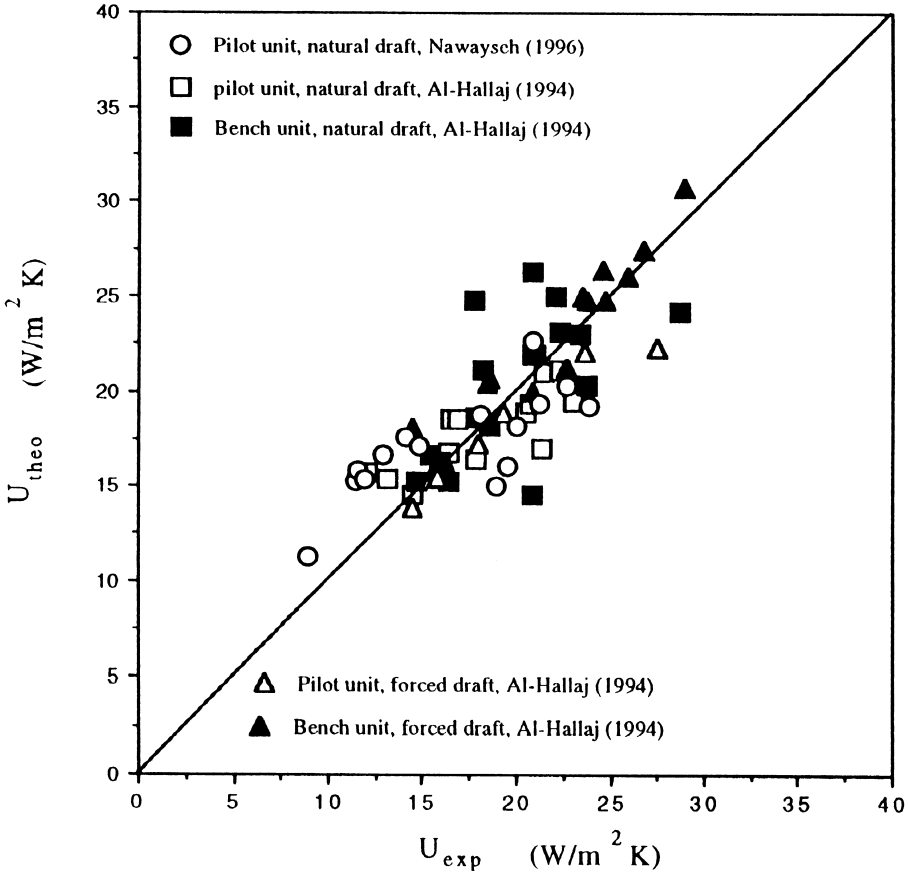

Fig. 10. Prediction of the overall heat transfer coefficient in the condensers of different designs.

The water side heat transfer coefficient was calculated from the known empirical correlation of flow in a pipe [12],

$$Nu_w = 0.023 Re^{0.8} Pr^{0.3} \tag{16}$$

The experimental values of the overall heat transfer coefficient U_{exp} were calculated from the heat load in the condenser:

$$LCp_w(T_2 - T_1) = U_{exp} A_c \left[\frac{(T_6 - T_2) - (T_5 - T_1)}{\ln \dfrac{T_6 - T_2}{T_5 - T_1}} \right] \tag{17}$$

The log-mean temperature difference between the humid air and the cooling water was used, even though the heat load–temperature relationship was non-linear in the condenser. The availability of a single value for the overall heat transfer coefficient would simplify the simulation of the unit. The coefficient, defined by Eqs. (9) and (13), is a function of the water flow rate, air flow rate and operating temperature. The air flow rate can not be increased, largely to avoid excessive pressure drop in the condenser and the humidifier. Hence, its effect on the heat transfer coefficient was found small, as may be seen from Eq. (7). Operating at higher temperature increased the overall heat transfer coefficient by reducing the condensation factor Z. Increasing the water flow rate not only increased the water side coefficient but also favorably affected the condition of the humid air coming from the humidifier. In the natural draft air circulation, increasing the water flow rate increased also the air velocity, creating a further increase in the overall coefficient.

Fig. 10 shows a plot of the calculated and measured overall heat transfer coefficient for the condensers used in the three units. The plot includes the data obtained from the measurements with natural and forced draft air circulation. The data lies within the 45° line, with a significant scatter which may be attributed to:

1. The vertical condensers of different geometry and design can not be assumed isothermal or smooth surfaces. Hence, the prediction of the convection coefficient from the air flowing along the condenser surface is highly inaccurate. There are no available correlations for similar cases.
2. The error involved in averaging the value of Z may be significant due to the large variation in the air temperature as it flows along the condenser. This is not so serious in the case of the forced draft where the variation in the air temperature is usually small; which may explain why most of the points of the forced draft measurements lie within the 45° line.

5. Conclusions

The humidification/dehumidification process was found suitable for the production of desalinated water using solar energy. Optimizing the design of such units requires computer simulation which, in turn, requires an accurate evaluation of the heat and mass transfer coefficients in the condenser and the humidifier. The effect of water flow rate was found significant on the heat and mass transfer coefficients in the condenser and the humidifier. The

effect of air flow rate was small, giving an indication that natural draft operation is preferable. The developed heat and mass transfer correlations for the condensers and humidifiers of different designs describe the effects of water flow rate, air flow rate, operating temperature and the geometry of the condenser and the humidifier.

Acknowledgements

The authors would like to acknowledge the experimental and computational facilities made available at both the Department of Chemical Engineering at Jordan University of Science and Technology and the School of Chemical Engineering at the University Sains Malaysia.

References

[1] Al-Hallaj S. Solar desalination by humidification–dehumidification cycle. MSc Thesis, Jordan University of Science and Technology, Jordan 1994.
[2] Nawayseh NK. Solar water desalination with natural draft air humidification–dehumidification process. MSc Thesis, University Sains Malaysia, Malaysia 1996.
[3] Heschl O, Sizman R. Solar desalination with recovery of heat of condensation. Tagungsbericht 5. Intern. Sonnenforum Berlin, Bd. 1, S. 375 1984.
[4] Sousa HJ, Janisch V. Solar desalination based on the multi-cycle concept. Desalination 1987;67:75–80.
[5] Assouad Y, Lavan Z. Solar desalination with latent heat recovery. Trans ASME 1988;110:14–6.
[6] Chaibi MT, Safi MJ, Hsairi M. Performance analysis of a solar desalination unit in South Tunisia. Desalination 1991;82:197–205.
[7] Khedr M. Techno-economic investigation of an air humidification–dehumidification desalination process. Chem Engng Technol 1993;16:270–4.
[8] Donald B. In: Cooling tower performance. New York: Chemical Publishing Co, 1984. p. 82,105.
[9] Hsieh JS. In: Solar energy engineering. New Jersey: Prentice-Hall, 1986. p. 110–47.
[10] Stoecker WF, Jones JW. In: Refrigeration & air conditioning, 2nd ed. Singapore: McGraw Hill, 1982. p. 418–9.
[11] Farid MM, Nawayseh NK, Al-Hallaj S, Timimi AR. Solar desalination with humidification dehumidification process: studies of heat and mass transfer. In: Proceeding of the Conference: SOLAR 95, Hobart, Tasmania, 1995. p. 293–306.
[12] Holman JP. In: Heat transfer, 7th ed. New Jersey: McGraw Hill, 1992. p. 282,365.
[13] Tanner DW, Pope D, Potter CJ, West D. Heat transfer in dropewise condensation of low pressure in the absence and presence of non-condensable gas. Int J Heat Mass Transfer 1968;11:181.
[14] Bell KJ, Ghaly MA. An approximate generalized design method for multicomponent/partial condenser. Ind Eng Chem 1973;69:6–13.